

Revised Research Article

Assessment of Forest above ground Biomass with SAR data using Linear Modeling in Joida Taluk, Uttara Kannada, India

Abstract

The study was conducted in Joida taluk of Uttara Kannada district to assess the forest aboveground biomass using L band data. In this study, an attempt was made to estimate the aboveground biomass using SAR backscatter. The study area covered dense, moderately dense, and sparse forests. Nearly 0.01 percent of the forest area was sampled through 30 sampling plots. The point center quadrate (PCQ) method was used to select the tree and collected the tree growth parameters viz., tree height, diameter at breast height (DBH), and diameter at the tree base. The sampling plots were randomly selected in all types of forest and the location details such as the latitude, longitude, and altitude were collected from GPS. The tree crown density was measured with a densitometer. Each sample plot of forest aboveground biomass (AGB) was estimated using specific gravity and field-measured forest parameters. The fully polarimetric quad-pol (HH, HV, VV & VH) space borne SAR data of the Phased Array L-band Synthetic Aperture Radar-2 (PALSAR-2) of Advanced Land Observing Satellite-2 (ALOS-2) is used in this study for the natural forest of Joida Taluk of Uttara Kannada, Karnataka, India. The Orthorectification was performed on the radiometrically calibrated SAR data to measure the normalized radar cross-section of all the field-measured forest plot locations. SAR backscatter-based Multiple Linear Regression (MLR) model was implemented to retrieve forest aboveground biomass of the study area. The cross-polarization (HV) had shown a good correlation with forest above ground biomass. Forest Stem Volume varies from 16.11 m³/ha to 1235.79m³/ha (12.88 t/ha to 1000.98 t/ha). The higher values are from the plots of dense forests having higher DBH and height. The sampled area included dense forest, moderately dense forest, and sparse forest and hence the variation in biomass has occurred. The Multiple Linear Regression (MLR) analysis was performed to estimate the aboveground biomass of the natural forest areas of the Joida taluk. This study used four combinations (HH & HV, VV & HH, HV & VH, VV & VH) of polarimetric channels in the forest aboveground biomass retrieval. Among them, the combination of HH and HV polarization shows a good correlation with field and predicted biomass. The predicted biomass from HH & HV polarisation varies from 79t/ha to 267t/ha, VV & VH shows the biomass from 62t/ha to 236t/ha, VV & HH showed from 62t/ha to 205 t/ha and HV & VH indicated from 79t/ha to 268t/ha. Among them the HH and HV polarization backscatter can be used to retrieve the aboveground biomass of forests through linear modeling. The RMSE and R² values that were obtained from the MLR for the polarimetric combinations HH & HV and HH & VV were 78 t/ha and 0.86, and 81 t/ha and 0.85 respectively. Forest AGB retrieval from HH & HV polarization-based MLR model has shown the best results. The results indicated that the backscatter from different polarisation could be used for developing the MLR model for estimating above ground biomass.

Keywords: Forest, Above ground Biomass, SAR, Polarization, Backscatter, Multiple Linear Regression (MLR)

1. Introduction

Forest plays a vital role in regulating climate through carbon sequestration in its biomass. Forest Aboveground Biomass (AGB) reflects the health and environmental conditions of a forest ecosystem (Sinha *et al.*, 2015). Forest is one of the important components of the ecosystem. Tropical forests are pivotal in this regard as they sequester and store relatively large amounts of carbon compared to other forests (Nesha *et al.*, 2020). Forest biomass is an essential component to index the condition of the forest. The forest is the major sink of carbon storage and it becomes the source due to anthropogenic activities leading to the degradation of forest which further leads to global warming (Zhu *et al.*, 2020). The accurate estimation of forest biomass is most important in estimating carbon storage. The importance of accurately reporting the carbon content (biomass) of forested lands over time has been acknowledged by several studies. It plays an irreplaceable role in mitigating global warming caused by the increase in atmospheric carbon dioxide. Forest AGB can be determined most robustly from the cross-polarimetric channel of L-band spaceborne SAR data. Recently, there has been growing interest in the use of spaceborne SAR data in estimating AGB of forest vegetation (Otakei & Emanuel, 2015). SAR sensor transmits a microwave pulse towards the Earth's surface and receives the backscattered signal that is determined by the surface and includes information regarding the land surface structure such as forest characteristics. Microwaves used in SAR remote sensing are not affected by cloud cover, hence SAR data is being widely used in areas where cloud cover exists for most of the period. SAR plays an important role in monitoring the biophysical parameters of forests since its microwave energy can penetrate clouds, which occur constantly in the tropics, and acquire data throughout the year (Lu 2006; Zhu *et al.* 2015 and Pham & Yoshino, 2017). The fully polarimetric quad-pol SAR data helps in identifying the ground features accurately from different combinations of polarization (HH, HV, VV, and VH) for land use and land cover classification (Garg *et al.* 2021, 2022; Verma *et al.* 2022). The HV polarization showed a good correlation with the biomass and the multi-linear regression model shows a good correlation between field calculated and predicted biomass (Behera *et al.* 2016; Sinha *et al.*, 2016; Mukhopadhyay *et al.* 2021). Several studies indicated that HV polarization is most suitable for predicting the biomass using backscatter. For estimating the biomass of forest, the backscatter from different polarization is very important as in quad-pol data, HV polarization gave better backscatter from the forest and backscatter intensity increases with the density of trees and AGB is increasing with the dense forest as indicated by higher backscatter from the dense forest. A stable relationship between SAR backscatter and above-ground biomass (AGB) has been observed and described in several studies (Behera *et al.* 2016; Joshi and Kumar 2017a; Mukhopadhyay *et al.* 2021; Stovall and Shugart, 2018). Many studies have reported signal saturation between 100 and 250 tons per hectare (t/ha) above which the measured SAR backscatter no longer increases proportionately. Polarimetric SAR remote sensing has shown wide applicability in forest parameters retrieval (Joshi and Kumar, 2017b; Khati *et al.* 2018; Kumar *et al.* 2017, 2018; Kumar *et al.*, 2020; Tomar *et al.* 2019). It has been found that the polarimetric SAR remote sensing (PolSAR) data is capable of providing information on contribution to backscattering from different contributors within the resolution cells and the polarimetric interferometric SAR (PolInSAR) technique has the potential to retrieve interferometric coherence contributed by different components of the manmade and natural targets (Asopa and Kumar, 2020; Babu *et al.*, 2022; Bhanu Prakash and Kumar, 2021a, 2021b; Shafai and Kumar, 2020). PolSAR-based forest aboveground estimation and PolInSAR-based forest height retrieval showed less dependency on field measurement for implementing modeling approaches with reasonable accuracy (Kumar *et al.*, 2020, 2019, 2017b, 2017a; Sai Bharadwaj *et al.*, 2015). However, collecting field data for the forest AGB estimation and taking measurements using stratified random sampling is not a very difficult task in

forest areas where there is not much diversity in forest types. For estimating the ground truth for aboveground biomass estimation of natural forest, point centered sampling method is most suitable as the tree spacing is not at regular intervals in a natural forest as compared to the line transect and square plot method. By keeping the above-mentioned points in mind, an experiment was planned to estimate the forest aboveground biomass using an L-band backscatter-based regression approach for the forest area of Joida taluk of Uttara Kannada district, Karnataka, India. The forest types of the Joida Taluk includes moist deciduous, Semi-evergreen, and evergreen forest with dense and moderately dense forest types based on crown density cover in each of the forest types. The biomass estimation from SAR data using MLR model-based approach for such a complex forest is very much challenging and rigorous. Hence an attempt was made to investigate the biophysical parameters of dense, moderately dense, and sparse forest areas using the point-centered quarter (PCQ) method. The point-centered quarter (PCQ) method is one of the most suitable sampling plans used in field-data collection for aboveground biomass measurement in natural forests with randomly spaced trees. The objectives of this research also include establishing a regression model for predicting the AGB of complex forests using backscatters of different polarisation of L-band spaceborne SAR data of the Phased Array L-band Synthetic Aperture Radar-2 (PALSAR-2) of Advanced Land Observing Satellite-2 (ALOS-2).

2. Materials and Methods

Study Area

The study area mainly covers the Joida (Supa) Taluk of Uttara Kannada, Western Ghats of Karnataka, India. It is located between the coordinates $14^{\circ} 54' 13''$ N to $15^{\circ} 31' 59''$ N latitude and $74^{\circ} 08' 11''$ E to $74^{\circ} 31' 10''$ E longitude with an elevation of 532m (Fig. 1). The mean monthly temperature ranges from 25°C to 33°C . The study area covered 2,87,000 hectares. It is mainly covered with dense forest; native vegetation is evergreen/semi-evergreen type and has a continuum to secondary/moist deciduous types in lower rainfall tracts to the east. Forest types in the study area were classified as tropical wet semi-evergreen and tropical moist deciduous forest types. The study area receives the tropical monsoon climate and the major tree species found are *Tectonagrandis*, *Xyliaxylocarpa*, *Lagerstroemia lanceolata*, *Terminalia bellirica*, *Terminalia paniculata*, *Dilleniapentagyna*, which are also found in the semi-evergreen and evergreen forest of other places (Sabzar Ahmad and Ramachandra, 2016). Fig. 1 shows the location of the study area on the Map of India. The political map of India that has been used in Fig. 1 is downloaded from the online map portal of the Survey of India (SoI) which is the National Survey and Mapping Organization of the country under the Department of Science & Technology. The green polygon in Fig. 1 is the state boundary map of Karnataka State, India. The Joida (Supa) Taluk of Uttara Kannada is shown in a yellow polygon in Fig. 1 and the rectangular shape (with dark yellow strips) over the Joida (Supa) Taluk shows the extent of the L-band ALOS-2 PALSAR-2 data.

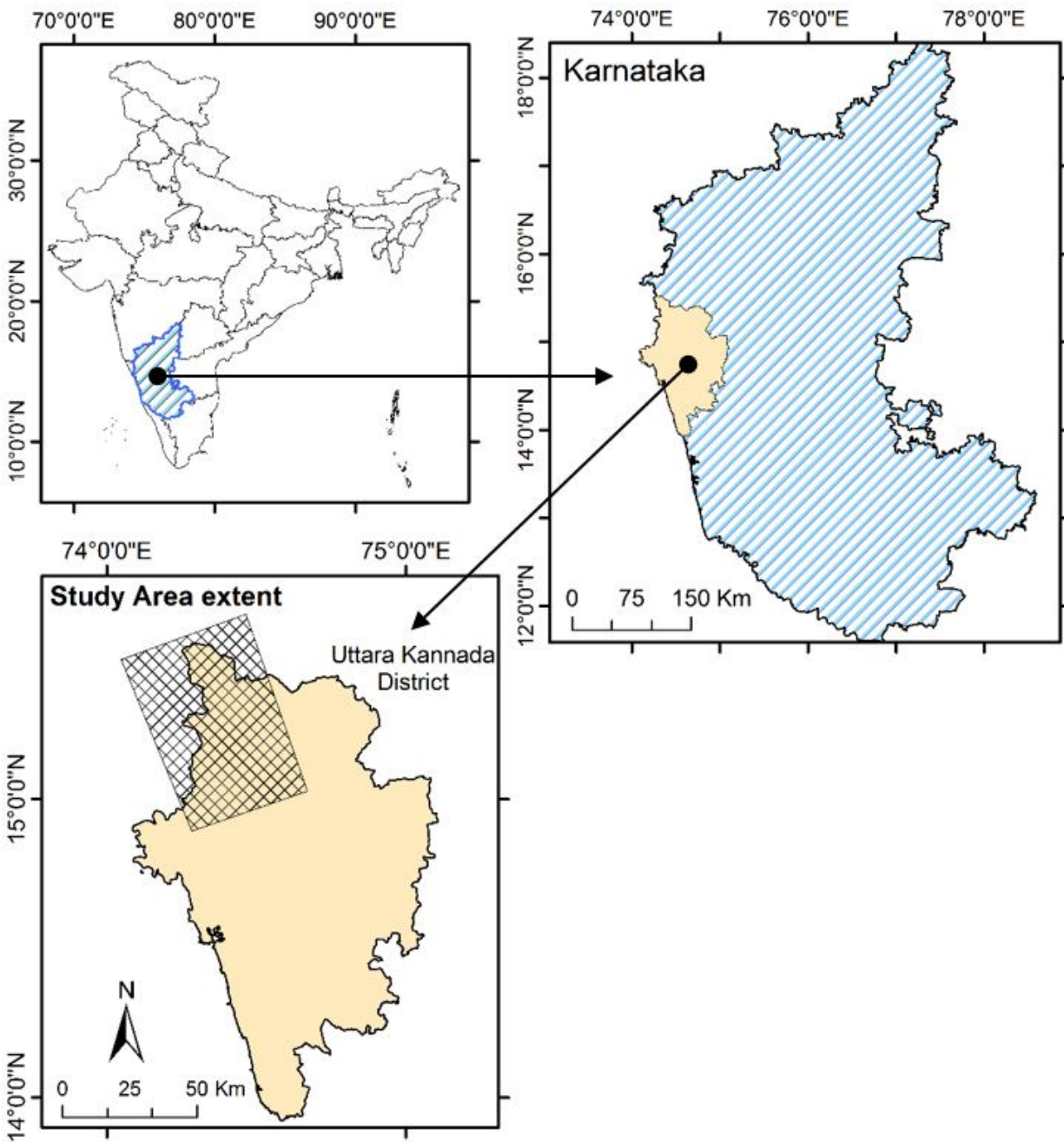


Fig.1 Study area map

Satellite Data Used:

The ALOS-2 PALSAR-2 single look complex (SLC) data was acquired on 26-05-2016 in strip map mode. The incidence angle of the quad-pol data was 38.97° . The data used was of 1.1 level which had the phase information. The L-band data is fully polarized having HH, HV, VH, and VV polarizations. A detailed description of the data is shown in Table 1.

Table: 1 Description of SAR data

Satellite/Sensor Name	ALOS-2 PALSAR-2
Date of Acquisition	26-05-2016
Range and Azimuth Resolutions	2.86 m and 3.11 m
Frequency and Wavelength	1236.499 MHz and 24.245 cm
Far and Near range Incidence Angles	37.619° and 40.284°
Polarizations	HH+HV+VH+VV

Field Data Collection

The field data from the study area were collected from the entire area using randomly selected sample plots. A total of 30 sample plots were laid out in the study area and the sampling plots of 30 numbers were approximately 0.01 percent of the forest area. Random field sampling plots were done throughout the study area according to accessibility. The Point Centered Quarter (PCQ) method was used to collect the data from the study area. The sample plots were taken in such a way that it represents the different forest density. In the PCQ method, 100 m length was randomly selected with the rope, and tree parameters were measured at starting point and at 25, 50, 75, and 100 m length. At each point, there are four quadrates in each quadrate one tree which is near the center was selected and a total of 4 trees one in each quadrate which is near the center point was selected, and its length from the center point was measured with a tape. The layout of the PCQ method is shown in Fig. 2. The PCQ method was used since this method is most suitable in the forest where the trees are randomly grown without proper spacing in a natural forest and the PCQ method is a more precise method for estimating the above-ground biomass (Kumarathunge *et al.*, 2011, Renske Hijbeek *et al.*, 2013, David *et al.* 2004). The distances of each tree from the center were recorded and tree growth parameters were recorded. The GBH (Girth at Breast Height), and girth at the base of the tree were measured with diameter tape. The height of the trees in the forest was measured with a Ravi multimeter made by Aqua Antiques Nauticals. The location of each sample plot information such as latitude/longitude and altitude were recorded using Garmin e Trex 20x GPS (Huang *et al.*, 2015). In each sample plot, a total of 20 trees were recorded and the sample area was estimated by multiplying the square of the average length of the trees from the center point (Total measured length /20) and the total number of trees (20). The tree volume was estimated using the standard formula given below (FRI 1996; Kasischke, & Christensen., 1990, Mangla *et al.*, 2016). The aboveground biomass was calculated after multiplying each tree's volume by its specific gravity (Kumar *et al.* 2012). The wood density or specific gravity that is represented by dry weight/green volume is the solid wood substance in a given volume of wood (Zobel, 2004).

$$\text{Stem Volume } SV = \text{Basal Area } BA \times \text{Tree Height} \times \text{Form Factor (FF)}$$

$$\text{Basal Area} = \pi(\text{DBH})^2/4$$

$$\text{Forest Aboveground Biomass (AGB)} = \text{Stem Volume } SV \times \text{Specific Gravity (SG)}$$

The artificial form factor (FF) is the ratio of the volume calculated using DBH and the tree volume calculated using the base diameter of the tree and is a unitless quantity.

PCQ Method : Point Centred Quarter Method

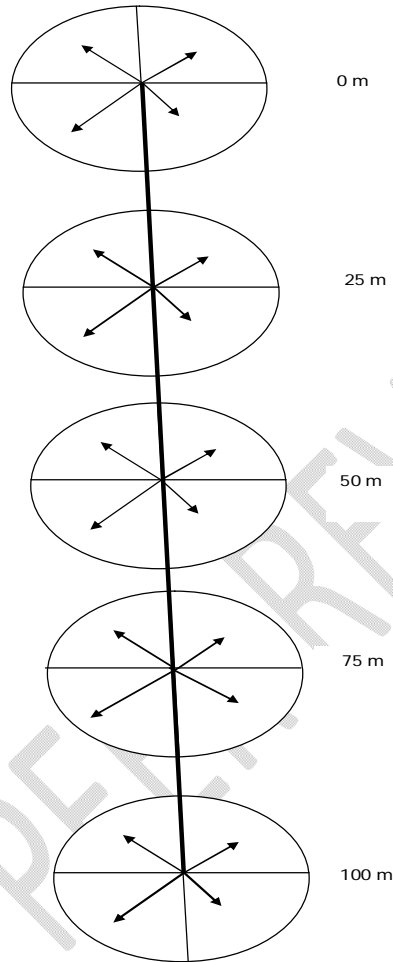


Fig.2 Sample plot design

The specific gravity of major species (FSI,1996) was considered and the average specific gravity for each sample plot was taken to obtain the aboveground biomass in tones(Chowdhury and Ghosh, 1958).

Satellite Data Analysis

The data used for the study was ALOS-2 PALSAR-2, L-band SAR data which is quad pol having all polarizations (HH, HV, VH, and VV). The data of each polarization contains real and imaginary bands (i and q) and intensity bands. These bands were used to create an RGB image. The data is being pre-processed and the methodology used is shown in the flowchart (Fig.3). The L band data was processed in the Sentinel-1 Toolbox (S1TBX) of Sentinel Application Platform (SNAP)V 8.0 (European Space Agency (ESA) 2020)and the radiometric calibration was performed to the single look complex (SLC) data of ALOS-2 PALSAR-2. Range-Doppler Terrain Correction algorithm was implemented on the quad-pol fully polarimetric SAR data for the Orthorectification using Copernicus 30m Global DEM in SNAP V 8.0 toolbox. A refined Lee filter was used to minimize the speckle effect from the SAR data.

The image was re-projected to the coordinate system of the study area (WGS_1984_UTM_Zone_43)(Das & Patnaik 2017; Das *et al.*, 2016; Sharifi *et al.*, 2016). The PALSAR-2 image was used to retrieve HH, HV, VV, and VH polarized backscatter coefficients which are expressed in decibels (dB). The data was calibrated to calculate the backscatter coefficient of the points where field data was collected. The backscatter calibration of SLC data of ALOS-2 PALSAR-2 was performed using Eq. (1) (Peregon& Yamagata., 2013). The backscatter cross-section of ALOS-2 PALSAR-2 can be obtained by the ensemble averaging or the spatial averaging of pixel values around the target as shown in Eq.(1) (Japan Aerospace Exploration Agency 2016).

$$\sigma_0 = 10 \times \log_{10} D N^2 + C F$$

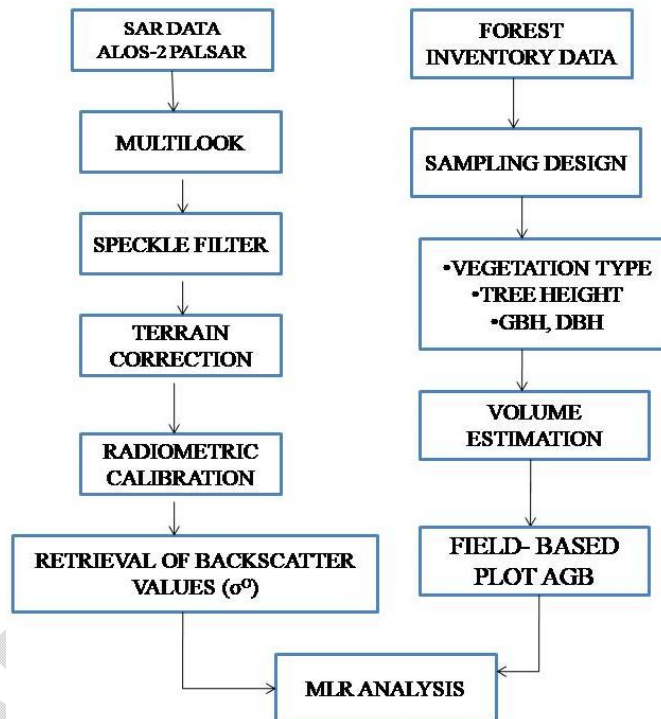


Fig. 3 Flowchart of methodology

Model Implementation

The study attempts to estimate forest AGB using field inventory data and geospatial techniques. A model was implemented for establishing the relationship between field inventory data and backscatter from different polarization. The individual relationship of each polarisation with field-measured AGB was used. The graphs were prepared between the field-generated AGB with the corresponding SAR backscattering coefficients.

The multilinear-linear regression analysis was done to relate the backscatter (σ^0) coefficient of SAR to the corresponding field calculated AGB. This model is used to analyze the relationship between the dependent variable (field measured forest AGB) and the independent variable (SAR backscatter)(Thumatyet *et al.*, 2016). This model regresses a correlated variable (AGB) based on one or more independent variables (Jha *et al.*, 2006; Zhu *et al.*, 2020). The growth parameters were collected from 30 PCQ sample plots out of which 20 plots of data were used for

model generation and the remaining 10 sample plots were used for model validation. The proportion of variance (R^2) and root mean square error (RMSE) is used to evaluate the model performance (Nizalpure et al., 2010). Eq. (2) is generated by using a common regression equation in which the model parameters were calculated by running the regression analysis between field calculated forest AGB and backscatter coefficients of the SAR data in different polarimetric combinations for the corresponding field plots.

$$Y_{\text{BIOMASS}(t/\text{ha})} = A + (B * \sigma^0_{\text{HH}}) + (C * \sigma^0_{\text{HV}}) \quad (2)$$

where A, B, and C are model parameters. The study carried out by Cassolet et al., 2019 had derived multiple linear regression models (MLR) equation between a dependent variable (Y) and multiple independent variables (backscatter coefficient). Many previous studies showed the use of the MLR model for estimating forest biomass by using the backscatter coefficient (Zhu et al., 2020; Das & Patnaik 2017).

Statistical Analysis

The regression model is validated by assessing the coefficient of determination (R^2) between the predicted and field-measured forest AGB values. The root mean square error was also calculated to know the relationship between observed and predicted values. The formula to calculate the RMSE is shown in Eq. (3).

$$\text{RMSE} = \sqrt{[\sum (P_i - O_i)^2 / n]} \quad (3)$$

Where \sum is the sum

P_i is the predicted value for i^{th} observation in the dataset.

O_i is the observed value for the i^{th} observation in the dataset.

n is the number of samples.

3. Results and discussion:

The aboveground biomass (AGB) of sampled plots was estimated in tones per hectare based on the sample plot biomass, the location of sample plots and corresponding biomass is given in Table 2.

Table: 2 Location of the field plots and field-measured forest parameters (Stem Volume and AGB)

Sl.no	Latitude	Longitude	Volume (m ³ /ha)	Aboveground Biomass (AGB) (t/ha)
1.	15°11'27"	74°29'71"	404.77	204.00
2.	15°11'17.89"	74°29'42"	122.00	98.82
3.	15°10'22.2"	74°29'08.9"	940.50	474.03
4.	15°10'30.38"	74°29'13.2"	722.43	585.16
5.	15°11'59.8"	74°31'61"	1235.79	1000.98
6.	15°8'46"	74°22'14"	502.03	330.33
7.	15°11'33.6"	74°32'38.8"	760.09	554.86

8.	15°11'8.7"	74°24'15.1"	333.92	219.71
9.	15°11'44"	74°31'42"	438.74	242.18
10.	15°10'46"	74°29'15"	628.00	413.22
11.	15°11'51"	74°31'36.6"	685.36	450.96
12.	15°10'39.7"	74°29'19.2"	290.17	190.93
13.	15°15'37.2"	74°14'9.1"	339.50	223.41
14.	15°10'15"	74°29'19"	802.51	585.83
15.	15°09'14"	74°28'0.28"	254.08	128.06
16.	15°09'21"	74°28'23"	270.42	136.29
17.	15°9'4.9"	74°35'15"	381.00	250.00
18.	15°11'18"	74°29'56"	287.00	173.00
19.	15°16'12"	74°18'5"	342.08	249.72
20.	15°20'12"	74°34'35"	144.56	86.74
21.	15°28'54"	74°29'41"	105.01	65.11
22.	15°20'71"	74°36'30"	226.59	149.09
23.	15°10'54"	74°29'51"	290.08	220.46
24.	15°11'94"	74°24'53"	77.40	62.70
25.	15°24'53"	74°29'51"	205.19	128.86
26.	15°12'54"	74°36'11"	152.72	122.18
27.	15°8'46"	74°29'51"	16.11	12.88
28.	15°08'22"	74°30'36"	35.59	17.93
29.	15°20'78"	74°28'11"	40.43	32.75
30.	15°11'72"	74°31'84"	378.22	109.70

Forest Stem Volume (SV) of sample plots varies from 16.11 m³/ha to 1235.79m³/ha. The higher values are from the plots of dense forests having higher DBH and height. The sampled area included dense forest, moderately dense forest, and sparse forest and hence the variation in biomass has occurred. Forest AGB of each sample plot in tones per hectare was varying from 12.88 t/ha to 1000.98 t/ha due to variations in the specific gravity of different species. An unexpectedly high forest AGB in sample plot 5 was due to large values of DBH and tree heights that were found in the evergreen forest whereas the lowest AGB found in the 27th plot was due to the small diameter tree and short height trees, since the PCQ method was followed randomly there was a chance of getting a uncertainty in field-measured forest parameters, hence there may be difference in AGB of forest patches. The backscatter of the L-band in different polarization from

different sample plots was used to predict the biomass. The backscatter image of HH, HV, VH, and VV is shown in Fig. 4.

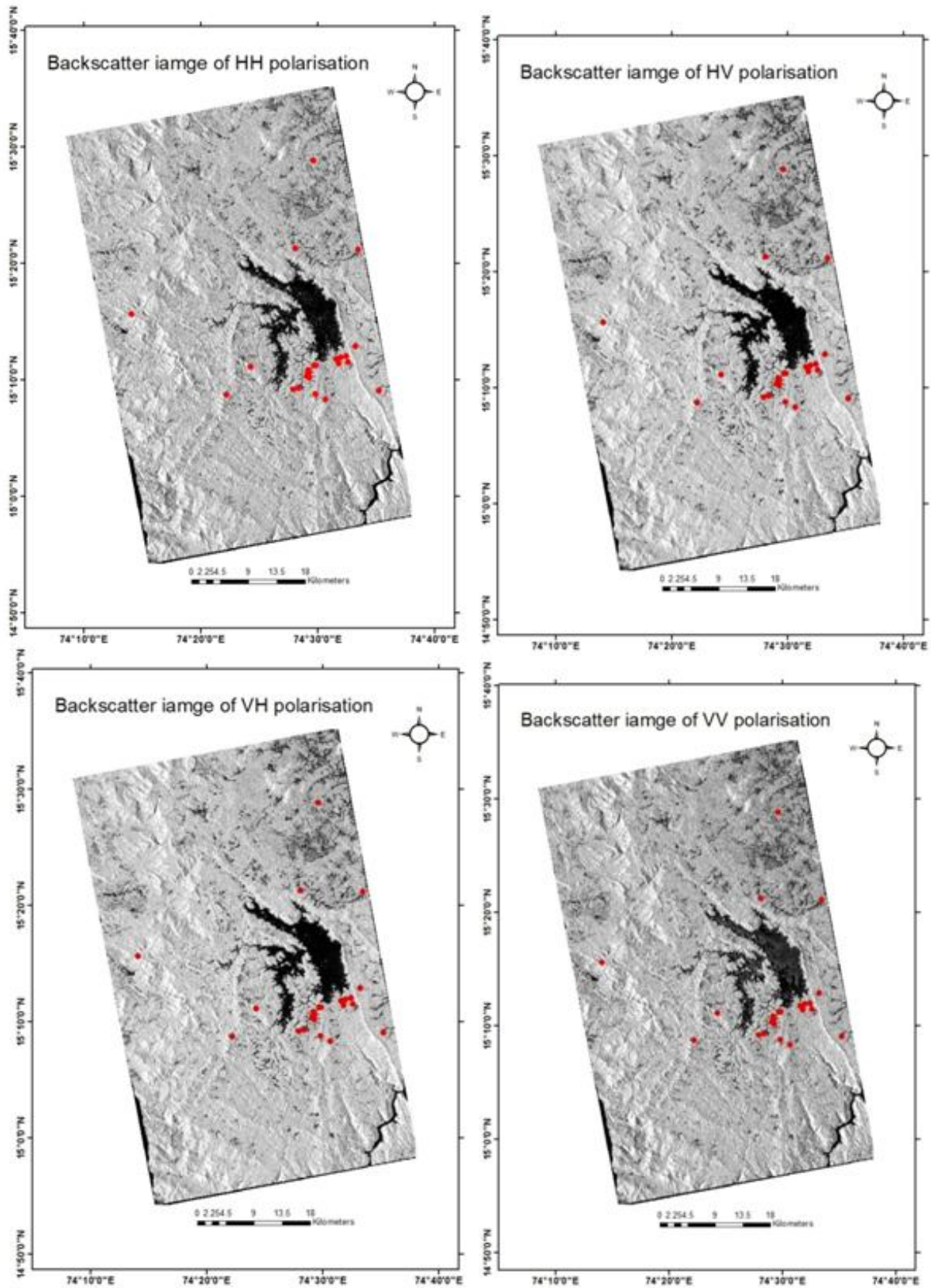


Fig. 4 Backscatter image of HH, HV, VH, and VV

Table: 3 The backscatter values (dB) for biomass plots from different polarization of the L band

SL NO	LAT	LONG	BIOMASS (t/ha)	HH	HV	VV	VH	Forest types
1	15°8'46"	74°29'51"	12.88	-8	-14	-9	-12	DF
2	15°08'22"	74°30'36"	17.93	-8	-15	-9	-12	O/SF
3	15°20'78"	74°28'11"	32.75	-7	-14	-8	-13	O/SF
4	15°11'94"	74°24'53"	62.70	-8	-14	-8	-13	O/SF
5	15°28'54"	74°29'41"	65.11	-6	-14	-9	-13	MDF
6	15°20'12"	74°34'35"	86.74	-6	-13	-9	-14	MDF
7	15°11'72"	74°31'84"	109.70	-8	-13	-10	-14	MDF
8	15°12'54"	74°36'11"	122.18	-6	-13	-8	-13	O/SF
9	15°09'14"	74°28'0.28"	128.06	-7	-13	-7	-13	DF
10	15°24'53"	74°29'51"	128.86	-6	-13	-7	-13	O/SF
11	15°09'21"	74°28'23"	136.29	-8	-14	-8	-14	DF
12	15°20'71"	74°33'30"	149.09	-7	-14	-11	-14	MDF
13	15°11'18"	74°29'56"	173.00	-6	-12	-6	-18	DF
14	15°10'39.7"	74°29'19.2"	190.93	-7	-11	-7	-13	MDF
15	15°11'27"	74° 29'71"	204.00	-8	-11	-7	-12	DF
16	15°11'8.7"	74°24'15.1"	219.71	-8	-12	-8	-12	O/SF
17	15°10'54"	74°29'51"	220.46	-7	-12	-6	-12	MDF
18	15°15'37.2"	74°14'9.1"	223.41	-5	-11	-5	-10	MDF
19	15°11'44"	74°31'42"	242.18	-6	-11	-6	-11	MDF
20	15°16'12"	74°18'5"	249.72	-6	-10	-3	-10	DF
21	15°20'12"	74°34'35"	249.72	-7	-12	-8	-11	MDF
22	15°9'4.9"	74°35'15"	250.00	-7	-11	-7	-11	DF
23	15°8'46"	74°22'14"	330.33	-7	-10	-6	-10	DF
24	15°10'46"	74°29'15"	413.22	-6	-11	-7	-11	MDF
25	15°11'51"	74°31'36.6"	450.96	-6	-10	-7	-10	MDF
26	15°10'22.2"	74°29'08.9"	474.03	-5	-11	-6	-11	MDF
27	15°11'33.6"	74°32'38.8"	554.86	-6	-11	-6	-11	MDF
28	15°10'15"	74°29'19"	585.83	-4	-9	-6	-11	MDF
29	15°11'17.89"	74°29'42"	818.00	-4	-9	-5	-12	MDF

30	15°11'59.8"	74°31'61"	1000.98	-3	-8	-4	-10	MDF
----	-------------	-----------	---------	----	----	----	-----	-----

DF=Dense forest MDF= Moderately dense forest O/SF= Open / sparse forest

The backscatter value depends upon the tree density, forest types, and AGB, as AGB increases the sar backscatter values also increases. The backscatter from HH polarization is varied from -8 to -3 dB. HV polarization is varies from -15 to -8 dB. VV polarization is varies from -11 to -3 dB. VH polarization is varied from -18 to -10 dB.

A polarimetrically calibrated SAR data of a monostatic SAR system shows the highly correlated scatterplot between the cross-polarimetric channels with similar/equal backscatter values for the corresponding locations in the image (Babu *et al.* 2021, 2022; Kumar *et al.* 2022; Maiti *et al.* 2021). The distortions from the PolSAR data are minimized with the polarimetric calibration exercise (Babu *et al.* 2019) and generally, the data provided to the users are free from errors and distortions (Kumar *et al.* 2022). Though deviation is observed in Fig. 5 for the backscatter values of HV and VH for a few plots, most of the plot locations' backscatter values of both the cross-polarimetric channels are the same. The correlation between backscatter values for different polarization against field calculated biomass is shown in Fig. 5. From Fig. 5 it is evident that the cross-polarimetric channel shows higher sensitivity toward forest AGB retrieval.

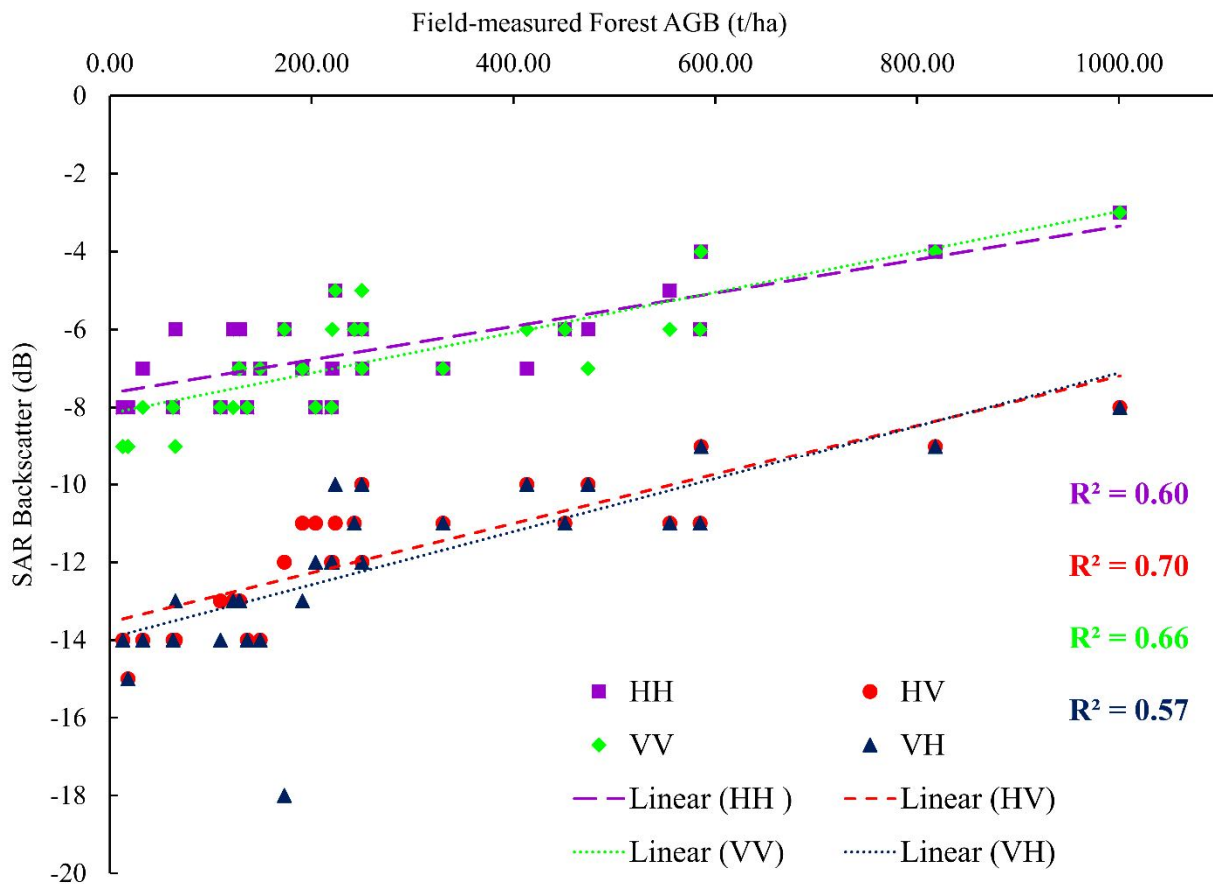


Fig.5 The correlation between calculated biomass and backscatter from different polarization

The backscatter values of HH and HV polarization versus biomass indicated the correlation value R^2 for HH is 0.60 whereas the correlation value for HV is 0.70. Similarly, the R^2 value for VV and VH are 0.66 and 0.57 respectively. Among the different polarization, the correlation of biomass w.r.t volume scattering (HV) is higher i.e 0.70. The HV polarization is mostly used for forest studies. Several studies show the HV polarization exhibit most of the volume scattering which results in a better correlation with field data (Behera *et al.* 2016; Sinha *et al.*,2016; Mukhopadhyay *et al.* 2021; Avtar *et al.*,2018). The vegetation scattering is dominant in HV polarization at a higher incidence angle because the backscatter depends on the volume of main scatterers (Le *et al.*, 2002). Cross-polarization is mostly suitable for backscatter retrieval from the forest vegetation. Since the volume scattering is dominant in cross-polarization it causes more backscattering in VH polarization.

Model Implementation

The ground truth data were collected from 30 sample plots across the study area. Based on the backscatter value for a different combination of polarization the predicted biomass was estimated. The predicted biomass obtained against the backscatter value w.r.t field calculated AGB is shown in Table 4. The 20 plots were used for model preparation and the remaining 10 plots were used for model validation. The 20 plots shown in Table 4 were used to retrieve the MLR model parameters. The model parameters are shown in Table 5 and these parameters are used in MLR for predicting the AFB of those plots which were used in the retrieval of model parameters A, B, and C.

Table 4 The field-measured AGB and predicted AGB

SL NO	Field calculated AGB(t/ha)	Predicted biomass (t/ha)			
		HH & HV	VV & VH	VV & HH	HV & VH
1	12.88	79	62	62	79
2	17.93	32	49	62	32
3	32.75	79	103	105	79
4	62.70	79	103	121	79
5	65.11	79	75	31	81
6	109.70	125	103	121	124
7	122.18	126	116	89	126
8	128.06	126	157	163	126
9	128.86	126	157	147	126
10	136.29	79	103	121	79
11	149.09	79	144	163	79
12	173.00	173	134	205	162
13	190.93	219	157	163	217
14	204.00	219	128	121	219
15	219.71	172	128	121	174
16	220.46	173	210	221	174
17	223.41	220	276	248	223

18	242.18	220	223	205	221
19	249.72	267	276	264	268
20	249.72	267	236	205	268

The predicted biomass using the backscattered coefficient was estimated. The equation for the biomass calculation is given in Eq. (2). The Multi-linear regression analysis is carried out by using the backscatter values for HH & HV, HH & VV, HV & VH, and VH & VV as given in Eq.(2) (Shao, & Zhang., 2016).

The model parameters A, B, and C, which were calculated during regression analysis are shown in Table 5. These model parameters were used to estimate forest AGB through the Multiple Linear Regression (MLR) model.

Table 5 Coefficients of MLR model's parameters

Polarisation	A	B	C
1. HH & HV	737	0.4	46
2. HH & VV	459	58	-15
3. HV & VH	740	45	2
4. VH & VV	608	40	12

The field calculated biomass varies from 13t/ha to 250t/ha. The predicted biomass from HH & HV polarisation varies from 79t/ha to 267t/ha, VV & VH shows the biomass varies from 62t/ha to 236t/ha, VV& HH showed the variation from 62t/ha to 205 t/ha and HV&VH indicated from 79t/ha to 268t/ha. The HH and HV polarization backscatter can be used to retrieve the aboveground biomass of forests. The cross-polarization backscatters are more sensitive for tree biomass estimation as compared to co-polarimetric backscatter values (Behera *et al.* 2016; Sinha *et al.*,2016; Mukhopadhyay *et al.* 2021; Preetilal *et al.*, 2021).

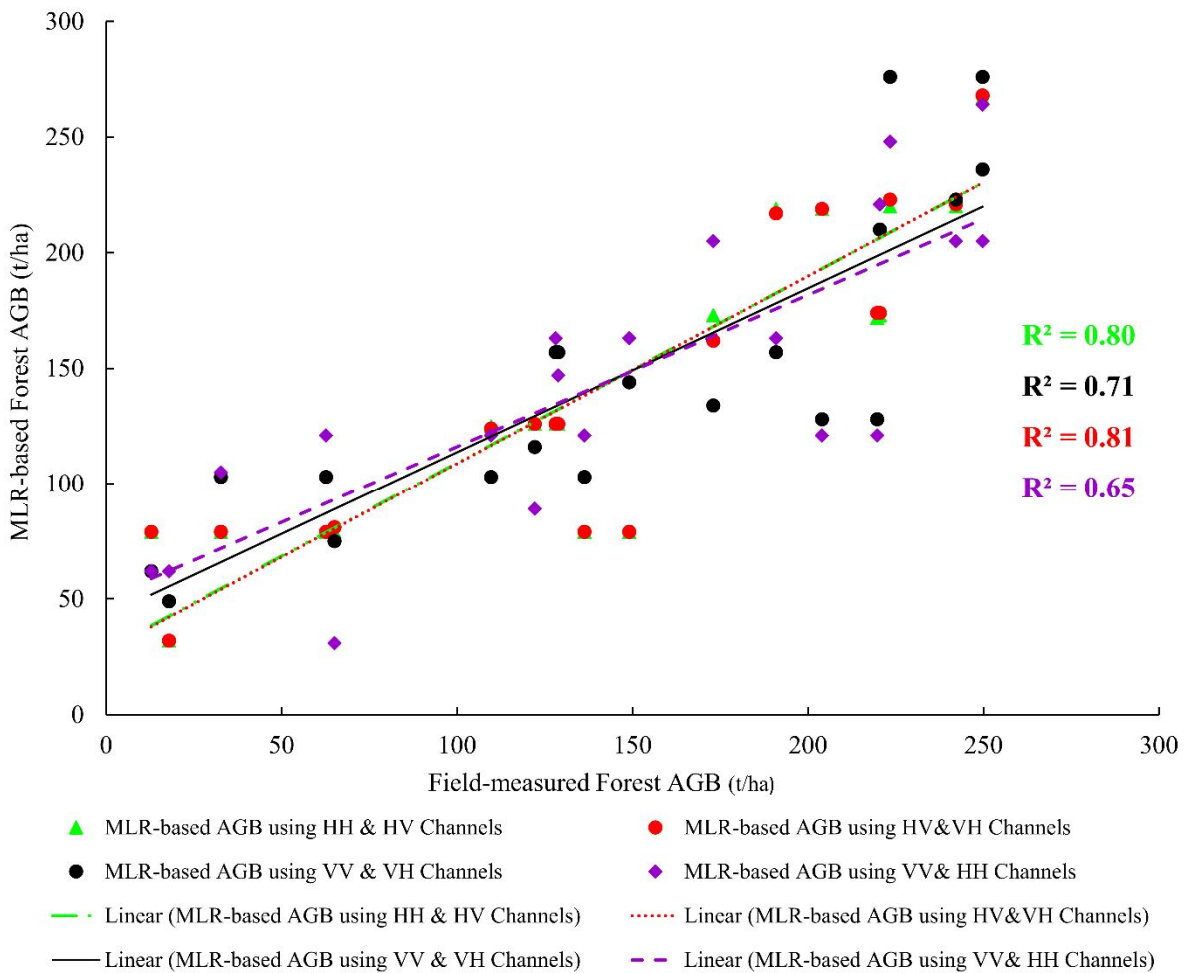


Fig. 6 Correlation between MLR predicted Forest AGB and Field-measured Forest AGB (t/ha) for those plots that were used to train the model in different polarimetric combinations of ALOS-2 PALSAR-2 data

Fig. 6 shows the correlation between the MLR-based forest AGB and field-measured forest AGB for those 20 plots that were used to train the model to retrieve the input parameters of the model. It is evident from Figure 6 that the highest coefficients of determinations were obtained from HH & HV and HV & VH polarimetric combinations. After analyzing the results shown in Fig. 6 it is clear that the MLR-based predicted forest AGB shows good agreement with field-measured forest AGB. Since the MLR model-based predicted AGB was compared with those forest plots that were used to train the model for input parameters retrieval so the remaining 10 plots of forest AGB were used for validation of the modeled output.

Model Validation

The model was validated by using the forest AGB values of the remaining 10 plots of the field-collected data. The Coefficients of MLR models that were retrieved for Eq.(2) are shown in Table 4. The validation of MLR was done with the help of field-collected forest AGB data for 10 plots. The validation was done for the different

polarimetric combinations of the ALOS-2 PALSAR-2 data. The coefficient of determination (R^2) and root mean square error (RMSE) was calculated for different polarimetric combinations and are given in Table 6.

Table: 6 RMSE and R^2 values of model validation

SL.NO	POLARISATION	RMSE	R^2
1	HH & HV	78 t/ha	0.86
2	HH & VV	81 t/ha	0.85
3	VH & VV	92 t/ha	0.81
4	HV & VH	115 t/ha	0.70

The four combinations of polarisation which are HH & HV, HH & VV, HV & VH, and VV & VH were used. The RMSE values range from 78 t/ha to 115 t/ha for different combinations. The HH & HV polarisation has the least RMSE value (78 t/ha). The analysis shows that the HH & HV showed the best correlation with R^2 at 0.86 followed by HH & VV with R^2 of 0.85, VH & VV R^2 of 0.81, and HV & VH R^2 of 0.70 respectively. The correlation between the predicted biomass and field calculated biomass for different polarimetric combinations is shown in Fig. 7. The 10 sample plots which were used for model validation and correlation for different combinations as shown in Fig. 7 have indicated that the correlation value is highest with HH and HV ($R^2=0.86$) followed by VV and VH ($R^2=0.81$). The lowest RMSE (78 t/ha) between field-collected forest AGB and model-derived output was obtained for the HH&HV polarimetric combination.

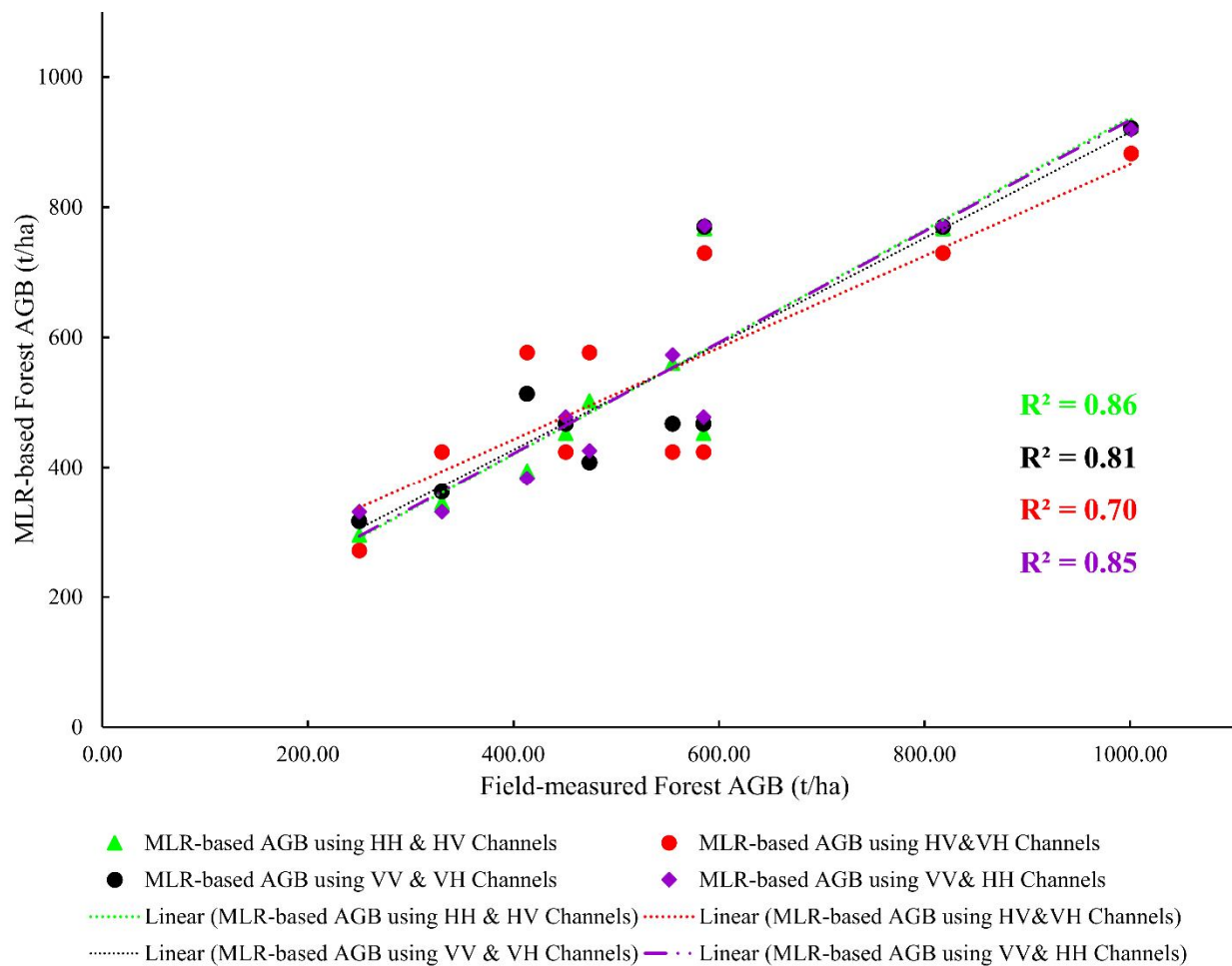


Fig. 7 Correlation between MLR predicted and Field-measured Forest AGB(t/ha) for different polarimetric combinations of ALOS-2 PALSAR-2 data

Discussion

A regression analysis was performed between the field-collected forest AGB values for the 30 plots and the corresponding backscatter values of the polarimetric channels (Fig. 5). A comparative analysis of the values of coefficient of determination (R^2) shows that the highest value is obtained for the cross polarimetric channel HV of the L-band ALOS-2 PALSAR-2 data. Higher ranges of backscatter values were obtained from like polarimetric combinations HH and VV, though comparatively low backscatter values were obtained in the L-band HV polarisation for the 30 plots of the field-measured forest AGB then also the best correlation was obtained with HV polarisation. The forest AGB of sample plots varied due to variation in DBH and height of trees. Since the sampled area covers dense forest, moderately dense forest, and sparse forest, crown density influenced the variation in growth parameters. The highest forest AGB of 1000.98 t/ha in the 5th plot (Table 2) was due to higher DBH and larger tree heights found in the evergreen forest. Since the sample plots were laid randomly hence such variation was found in one plot in a real situation it could have happened. The very low AGB in the 27th plot was due to the small diameter tree and less tree height (Table 2). This is one of the drawbacks of the PCQ method since the line transect was laid randomly it is the chance factor that there is the possibility of getting big trees and very small trees in any of the quadrates at every 25 meters. Among the different polarisations, the backscatter from HH and VV was higher

(-3 dB) whereas the highest backscatter from cross polarisation both HV and VH were -8 and -10 respectively. However, saturation in backscatter was observed in several studies (Mermozet *et al.* 2015) but in the present study, a clear saturation in SAR backscatter and forest AGB was not detected. This may be due to the small number of field plots in each forest type as a total of 30 plots were selected for different forest types which is a very small number for such a heterogeneous forest area. The uncertainty in positional accuracy of the field measured plots could also be not avoided as a reason for not getting a saturation in SAR backscatter and forest AGB. Several studies have shown that the HV polarization exhibit most of the volume scattering which results in better correlation with field data (Englhart *et al.*, 2011; Behera *et al.* 2016; Sinha *et al.*, 2016; Mukhopadhyay *et al.* 2021; Avtar *et al.*, 2018). The vegetation scattering is dominant in HV polarization at a higher incidence angle because the backscatter is contributed by the volume of the vegetation (Le *et al.*, 2002). The cross-polarization is volumetric scattering which is most suitable for the forest.

The MLR was validated and it was found that the coefficient of determination (R^2) was varying from 0.70- to 0.86 for different polarimetric combinations. The polarimetric combination HH & HV has shown the best predicted MLR-based forest AGB in comparison to HV&VH, VV & VH, and HH & VV. The coefficient of determination that was obtained from HH & HV MLR-based forest AGB was 0.86 which shows an approximately 0.93 correlation coefficient. The root mean square error (RMSE) for the MLR-based modeled forest AGB was minimum for the same polarimetric combination. The reason for getting the best values with HH & HV based MLR for forest AGB retrieval may be due to the sensitivity of the HH polarization to the double bounce scattering due to the tree trunks (Herndon *et al.* 2020) and the sensitivity of the HV polarization to the volumetric scattering due to the multiple reflections from the tree canopy, twigs, and branches. The model has also been used for predicting the AGB for the vegetation of moist and semi-evergreen forests. The main limitation of the MLR model, which is used for measuring the forest AGB of different vegetation types, is that the polarimetric combinations of the SAR data should have backscatter values ranging between -3 dB to -18 dB. The backscatter values >-3 and less than -18 dB of different polarimetric combinations of the SAR data are not suitable input values in the MLR for predicting the forest AGB.

Conclusion

The main objective of this research was the evaluation of the potential of fully polarimetric L- band space borne SAR data in the MLR for estimating the vegetation AGB of complex forests. Point Centered Quarter (PCQ) sampling method was used for collecting the field data for 30 different locations of different forest types in the study area. The results indicated that out of 30 plots 7 plots are having AGB less than 100 t/ha and 7 plots are having values greater than 400 t/ha. Out of the 7 plots that are having AGB greater than 400 t/ha, one plot is having AGB value greater than 1000 t/ha which is unexpectedly very high. The scatterplot between the polarimetric channels and the field-measured forest AGB data for the 30 plots shows that the highest coefficient of determination is obtained from the HV polarization. The different backscatter values in HV and VH polarisations were observed for 5 plots and for the remaining 25 plots the backscatter values in both the polarimetric channels are similar. The very high AGB for the plot is due to the large DBH and forest height in the forest plot. The 20 forest plots that were used in the MLR parameters retrieval, the model-based AGB values for the same plots were retrieved and compared with the field-measured data. A good correlation was obtained between field-measured forest AGB and MLR model-based

predicted forest AGB for those 20 plots that were used in the model training. The validation of the modeling approach was performed with the 10 remaining plots that were not used in the model training and it was observed that the highest coefficient of determination with the lowest RMSE was obtained with HH & HV polarimetric combination. The study recommends the implementation of the MLR model for forest AGB retrieval using a time-series approach of multi frequency data to minimize any season-induced uncertainty in the forest vegetation.

Disclaimer: No generative AI technologies such as large language Models (chat GPT COPILOT etc) and text to image generators have been used during writing or editing of this manuscripts

Reference:

- Asopa, U., Kumar, S., 2020. UAVSAR Tomography for Vertical Profile Generation of Tropical Forest of Mondah National Park, Gabon. *Earth Sp. Sci.* 7, e2020EA001230; 1-14. <https://doi.org/10.1029/2020EA001230>
- Avtar, R., Mukherjee, S., Abayakoona, S. B. S., Sophal, C., &Thapad, R. (2018). Integrating ALOS-PALSAR and ground based observations for forest biomass estimation for REDD+ in Cambodia. *APN Science Bulletin*, 8(1), 52-58.doi.org/10.30852/sb.2018.414.
- Babu, A., Kumar, S., & Agrawal, S. (2019). Polarimetric Calibration of RISAT-1 Compact-Pol Data. *IEEE Journal of Selected Topics in Applied Earth Observations and Remote Sensing*, 12(10), 3731–3736. <https://doi.org/10.1109/jstars.2019.2932019>
- Babu, A., Kumar, S., & Agrawal, S. (2021). Polarimetric Calibration of L-Band UAVSAR Data. *Journal of the Indian Society of Remote Sensing*, 49(3), 541–549. <https://doi.org/10.1007/s12524-020-01241-1>
- Babu, A., Kumar, S., & Agrawal, S. (2022). Polarimetric Calibration and Spatio-temporal Polarimetric Distortion Analysis of UAVSAR PolSAR data. *Earth and Space Science*, 9(4), e2020EA001629: 1-16. <https://doi.org/10.1029/2020EA001629>
- Behera, M.D., Tripathi, P., Mishra, B., Kumar, S., Chitale, V.S., Behera, S.K., 2016. Above-ground biomass and carbon estimates of Shorearobusta and Tectonagrandis forests using QuadPOL ALOS PALSAR data. *Adv. Sp. Res.* 57, 552–561. <https://doi.org/10.1016/j.asr.2015.11.010>
- Bhanu Prakash, M.E., Kumar, S., 2021a. PolInSAR decorrelation-based decomposition modelling of spaceborne multifrequency SAR data. *Int. J. Remote Sens.* 42, 1398–1419. <https://doi.org/10.1080/01431161.2020.1829155>
- Bhanu Prakash, M.E., Kumar, S., 2021b. Multifrequency Analysis of PolInSAR-based Decomposition using Cosine-Squared Distribution. *IETE Tech. Rev.* 1–8. <https://doi.org/10.1080/02564602.2021.1892542>
- Cassol, H. L. G., Carreiras, J. M. D. B., Moraes, E. C., Silva, C. V. D. J., Quegan, S., & Shimabukuro, Y. E. (2019). Retrieving secondary forest aboveground biomass from polarimetric ALOS-2 PALSAR-2 data in the Brazilian Amazon. *Remote Sensing*, 11(1), 59.doi.org/10.3390/rs11010059.

- Das, A. K., & Patnaik, C. (2017). Monitoring Forest Above-Ground Biomass of Gujarat State Using Multi-Temporal Synthetic Aperture Radar Data. Paper presented in the *38th Asian Conference on Remote Sensing*, October 23-27, New Delhi (INDIA)
- Das, A., Patnaik, C., Pandey, D., & Maity, S. (2016). Estimation of Forest Above-Ground Biomass over Different Vegetation Types in India Using SAR Data. Paper presented in the *10th SPIE Asia-Pacific Remote Sensing symposium* held in Delhi during 04-07 April 2016. <https://doi.org/10.1109/36.134090>.
- Englhart S, Keuck V, Siegert F. (2011). Aboveground biomass retrieval in tropical forests—The potential of combined X-and L-band SAR data use. *Remote sensing of environment*. 115(5),1260-71.
- European Space Agency (ESA). (2020). Sentinel Application Platform (SNAP): Sentinel-1 Toolbox (S1TBX). European Space Agency (ESA). <http://step.esa.int/main/download/snap-download/>
- Garg, R., Kumar, A., Bansal, N., Prateek, M., & Kumar, S. (2021). Semantic Segmentation of PolSAR image data using Advanced Deep Learning Model. *Scientific Reports*, 11, 15365:1–18. <https://doi.org/10.1038/s41598-021-94422-y>
- Garg, R., Kumar, A., Prateek, M., Pandey, K., & Kumar, S. (2022). Land Cover Classification of Spaceborne Multifrequency SAR and Optical Multispectral Data using Machine Learning. *Advances in Space Research*, 69(4), 1726–1742. <https://doi.org/10.1016/j.asr.2021.06.028>
- Herndon, K., Meyer, F., Flores, A., Cherrington, E., Kucera, L., & Earth Science Data Systems. (2020). What is Synthetic Aperture Radar? <https://earthdata.nasa.gov/learn/backgrounders/what-is-sar>. Accessed 3 January 2022
- Huang, W., Sun, G., Ni, W., Zhang, Z., & Dubayah, R. (2015). Sensitivity of multi-source SAR backscatter to changes in forest aboveground biomass. *Remote Sensing*, 7(8), 9587-9609. doi: 10.3390/rs70809587.
- Joshi, S. K., & Kumar, S. (2017a). Performance of PolSAR backscatter and PolInSAR coherence for scattering characterization of forest vegetation using single pass X-band spaceborne synthetic aperture radar data. *Journal of Applied Remote Sensing*, 11(2), 026022. <https://doi.org/10.1117/1.jrs.11.026022>
- Joshi, S.K., Kumar, S., (2017b). Spaceborne PolInSAR tomography for vertical profile retrieval of forest vegetation. *J. Appl. Remote Sens.* 11, 016001. <https://doi.org/10.1117/1.jrs.11.016001>
- Khati, U., Singh, G., & Kumar, S. (2018). Potential of Space-Borne PolInSAR for Forest Canopy Height Estimation Over India—A Case Study Using Fully Polarimetric L-, C-, and X-Band SAR Data. *IEEE Journal of Selected Topics in Applied Earth Observations and Remote Sensing*, 11(7), 2406–2416. <https://doi.org/10.1109/JSTARS.2018.2835388>
- Kumar, S., Khati, U. G., Chandola, S., Agrawal, S., & Kushwaha, S. P. S. (2017). Polarimetric SAR Interferometry based modeling for tree height and aboveground biomass retrieval in a tropical deciduous forest. *Advances in Space Research*, 60(3), 571–586. <https://doi.org/10.1016/j.asr.2017.04.018>
- Kumar, S., Sara, R., Singh, J., Agrawal, S., & Kushwaha, S. P. S. (2018). Spaceborne PolInSAR and ground-based TLS data modeling for characterization of forest structural and biophysical parameters. *Remote Sensing Applications: Society and Environment*, 11(April), 241–253. <https://doi.org/10.1016/j.rsase.2018.07.010>
- Kumar, S., Garg, R.D., Govil, H., Kushwaha, S.P.S., 2019. PolSAR-decomposition-based extended water cloud modeling for forest aboveground biomass estimation. *Remote Sens.* 11, 1–27. <https://doi.org/10.3390/rs11192287>

- Kumar, S., Garg, R.D., Kushwaha, S.P.S., Jayawardhana, W.G.N.N., Agarwal, S., 2017a. Bistatic PolInSAR Inversion Modelling for Plant Height Retrieval in a Tropical Forest. *Proc. Natl. Acad. Sci. India Sect. A - Phys. Sci.* 87, 817–826. <https://doi.org/10.1007/s40010-017-0451-9>
- Kumar, S., Garg, R.D., Kushwaha, S.P.S., Pandey, U., 2017b. Spaceborne SAR Tomography for Vertical Profile Retrieval of Forest Vegetation. *Proc. Natl. Acad. Sci. India Sect. A - Phys. Sci.* 87, 807–816. <https://doi.org/10.1007/s40010-017-0450-x>
- Kumar, S., Govil, H., Srivastava, P.K., Thakur, P.K., Kushwaha, S.P.S., 2020. Spaceborne Multifrequency PolInSAR-Based Inversion Modelling for Forest Height Retrieval. *Remote Sens.* 12, 1–27. <https://doi.org/10.3390/rs12244042>
- Kumar, S., Babu, A., Agrawal, S., Asopa, U., Shukla, S., & Maiti, A. (2022). Polarimetric Calibration of Spaceborne and Airborne Multifrequency SAR Data for Scattering-Based Characterization of Manmade and Natural Features. *Advances in Space Research*, 69(4), 1684–1714. <https://doi.org/https://doi.org/10.1016/j.asr.2021.02.023>
- Lu, D. (2006). “The potential and challenge of remote sensing-based biomass estimation,” *Int. J. Remote Sens.* 27, 1297–1328
- Maiti, A., Kumar, S., Tolpekin, V. A., & Agarwal, S. (2021). A Computationally Efficient Hybrid Framework for Polarimetric Calibration of Quad-Pol SAR Data. *Earth and Space Science*, 8(3), e2020EA001447:1-22. <https://doi.org/10.1029/2020EA001447>
- Mangla, Rohit, Shashi Kumar, and Subrata Nandy., (2016). “Random forest regression modelling for forest aboveground biomass estimation using RISAT-1 PolSAR and terrestrial LiDAR data.” In *Lidar Remote Sensing for Environmental Monitoring XV*, International Society for Optics and Photonics. 9879: 98790Q. doi: 10.1117/12.2227380.
- Mermoz, S., Réjou-Méchain, M., Villard, L., Le Toan, T., Rossi, V., & Gourlet-Fleury, S. (2015). Decrease of L-band SAR backscatter with biomass of dense forests. *Remote Sensing of Environment*, 159, 307–317. <https://doi.org/https://doi.org/10.1016/j.rse.2014.12.019>
- Mukhopadhyay, R., Kumar, S., Aghababaei, H., Kulshrestha, A., 2021. Estimation of aboveground biomass from PolSAR and PolInSAR using regression-based modelling techniques. *Geocarto Int.* 0, 1–27. <https://doi.org/10.1080/10106049.2021.1878289>
- Nesha, M. K., Hussin, Y. A., van Leeuwen, L. M., & Sulistioadi, Y. B. (2020). Modeling and mapping aboveground biomass of the restored mangroves using ALOS-2 PALSAR-2 in East Kalimantan, Indonesia. *International Journal of Applied Earth Observation and Geoinformation*, 91, 102158. doi.org/10.1016/j.jag.2020.102158.
- Otukei, J. R., & Emanuel, M. (2015). Estimation and mapping of above ground biomass and carbon of Bwindi impenetrable National Park using ALOS PALSAR data. *South African Journal of Geomatics*, 4(1), 1-13. doi: 10.4314/sajg.v4i1.1.
- Pham, T. D., & Yoshino, K. (2017). Aboveground biomass estimation of mangrove species using ALOS-2 PALSAR imagery in Hai Phong City, Vietnam. *Journal of Applied Remote Sensing*, 11(2), 026010. doi.org/10.1117/1.JRS.11.026010
- Pham, T. D., K. Yoshino, and D. T. Bui, (2016) “Biomass estimation of *Sonneratiacaseolaris* (L.)Engler at a coastal area of Hai Phong city (Vietnam) using ALOS-2 PALSAR imagery and GIS-based multi-layer perceptron neural networks,” *GISci. Remote Sens.* 53(3), 1–25. DOI: 10.1080/15481603.2016.1269869
- Preet Lal, Amit Kumar, PurabiSaikia, Anup Das, C. Patnaik, Gajendra Kumar, A. C. Pandey, Parul Srivastava, C. S Dwivedi & M. L. Khan(2021)Effect of vegetation structure on above ground biomass in tropical deciduous forests of Central India, Geocarto International, DOI: [10.1080/10106049.2021.1936213](https://doi.org/10.1080/10106049.2021.1936213).

- Sabzar Ahmad Kuchay & Ramachandra, T. V. (2016). Land Use Land Cover Change Analysis of Uttara Kannada. *Imperial Journal of Interdisciplinary Research (IJIR)*, 2(4), 460-471.
- Sai Bharadwaj, P., Kumar, S., Kushwaha, S.P.S., Bijker, W., 2015. Polarimetric scattering model for estimation of above ground biomass of multilayer vegetation using ALOS-PALSAR quad-pol data. *Phys. Chem. Earth* 83–84, 187–195. <https://doi.org/10.1016/j.pce.2015.09.003>
- Shafai, S.S., Kumar, S., 2020. PolInSAR Coherence and Entropy-Based Hybrid Decomposition Model. *Earth Sp. Sci.* 7, e2020EA001279: 1-17. <https://doi.org/10.1029/2020ea001279>
- Shao, Z., & Zhang, L. (2016). Estimating forest aboveground biomass by combining optical and SAR data: a case study in Genhe, Inner Mongolia, China. *Sensors*, 16(6), 834. doi.org/10.3390/s16060834.
- Sharifi, A., Amini, J., & Tateishi, R. (2016). Estimation of forest biomass using multivariate relevance vector regression. *Photogrammetric Engineering & Remote Sensing*, 82(1), 41-49. doi.org/10.14358/PERS.83.1.41.
- Sinha, S., Jeganathan, C., Sharma, L. K., & Nathawat, M. S. (2015). A review of radar remote sensing for biomass estimation. *International Journal of Environmental Science and Technology*, 12(5), 1779-1792. [doi: 10.1007/s13762-015-0750-0](https://doi.org/10.1007/s13762-015-0750-0)
- Sinha, S., Jeganathan, C., Sharma, L. K., Nathawat, M. S., Das, A. K., & Mohan, S. (2016). Developing synergy regression models with space-borne ALOS PALSAR and Landsat TM sensors for retrieving tropical forest biomass. *Journal of Earth System Science*, 125(4), 725-735. [doi. 10.1007/s12040-016-0692-z](https://doi.org/10.1007/s12040-016-0692-z).
- Stovall A. E. and H. H. Shugart, (2018). “Improved biomass calibration and validation with terrestrial LIDAR: implications for future LIDAR and SAR missions,” *IEEE J. Sel. Top. Appl. Earth Obs. Remote Sens.* 11(10), 3527–3537.
- Thumaty, K. C., Fararoda, R., Middinti, S., Gopalakrishnan, R., Jha, C. S., & Dadhwal, V. K. (2016). Estimation of above ground biomass for central Indian deciduous forests using ALOS PALSAR L-band data. *Journal of the Indian Society of Remote Sensing*, 44(1), 31-39. [doi: 10.1007/s12524-015-0462-4](https://doi.org/10.1007/s12524-015-0462-4).
- Tomar, K. S., Kumar, S., & Tolpekin, V. A. (2019). Evaluation of Hybrid Polarimetric Decomposition Techniques for Forest Biomass Estimation. *IEEE Journal of Selected Topics in Applied Earth Observations and Remote Sensing*, 12(10), 3712–3718. <https://doi.org/10.1109/JSTARS.2019.2947088>
- Verma, S., Kumar, S., Mishra, V. N., & Raj, R. (2022). Multifrequency Spaceborne SAR data for Backscatter-based Characterization of Land Use and Land Cover. *Frontiers in Earth Science*, 10, 825255:1–24. <https://doi.org/10.3389/feart.2022.825255>
- Zhu Y. *et al.* (2015), “Retrieval of mangrove aboveground biomass at the individual species level with worldview-2 images,” *Remote Sens.* 7, 12192–12214
- Zhu, Y., Feng, Z., Lu, J., & Liu, J. (2020). Estimation of forest biomass in Beijing (China) using multisource remote sensing and forest inventory data. *Forests*, 11(2), 163. doi.org/10.3390/f11020163.
- Zobel, B., 2004. Tree Breeding, Practices | Biological Improvement of Wood Properties, in: Burley, J. (Ed.), *Encyclopedia of Forest Sciences*. Elsevier, Oxford, pp. 1458–1466. [https://doi.org/https://doi.org/10.1016/B0-12-145160-7/00038-7](https://doi.org/10.1016/B0-12-145160-7/00038-7)